Article

Mechanistic Studies of the Copolymerization Reaction of Oxetane and Carbon Dioxide to Provide Aliphatic Polycarbonates Catalyzed by (Salen)CrX Complexes

Donald J. Darensbourg, Adriana I. Moncada, Wonsook Choi, and Joseph H. Reibenspies

J. Am. Chem. Soc., **2008**, 130 (20), 6523-6533 • DOI: 10.1021/ja800302c • Publication Date (Web): 29 April 2008

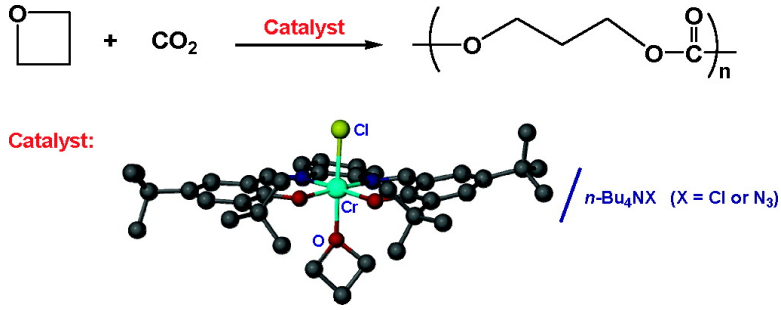

More About This Article

Additional resources and features associated with this article are available within the HTML version:

- Supporting Information
- Links to the 1 articles that cite this article, as of the time of this article download
- Access to high resolution figures
- Links to articles and content related to this article
- Copyright permission to reproduce figures and/or text from this article

View the Full Text HTML

J|A|C|S
ARTICLES

Published on Web 04/29/2008

Mechanistic Studies of the Copolymerization Reaction of Oxetane and Carbon Dioxide to Provide Aliphatic Polycarbonates Catalyzed by (Salen)CrX Complexes

Donald J. Darensbourg,* Adriana I. Moncada, Wonsook Choi, and Joseph H. Reibenspies

Department of Chemistry, Texas A&M University, College Station, Texas 77843

Received January 14, 2008; E-mail: djdarens@mail.chem.tamu.edu

Abstract: Chromium salen derivatives in the presence of anionic initiators have been shown to be very effective catalytic systems for the selective coupling of oxetane and carbon dioxide to provide the corresponding polycarbonate with a minimal amount of ether linkages. Optimization of the chromium(III) system was achieved utilizing a salen ligand with *tert*-butyl groups in the 3,5-positions of the phenolate rings and a cyclohexylene backbone for the diimine along with an azide ion initiator. The mechanism for the coupling reaction of oxetane and carbon dioxide has been studied. Based on binding studies done by infrared spectroscopy, X-ray crystallography, kinetic data, end group analysis done by ^{1}H NMR, and infrared spectroscopy, a mechanism of the copolymerization reaction is proposed. The formation of the copolymer is shown to proceed in part by way of the intermediacy of trimethylene carbonate, which was observed as a minor product of the coupling reaction, and by the direct enchainment of oxetane and CO_2. The parity of the determined free energies of activation for these two processes, namely 101.9 kJ·mol^{-1} for ring-opening polymerization of trimethylene carbonate and 107.6 kJ·mol^{-1} for copolymerization of oxetane and carbon dioxide supports this conclusion.

Introduction

The utilization of carbon dioxide in the production of value-added chemicals has received intense scrutiny over the past decade.[1] This is a consequence of carbon dioxide being an abundant, nontoxic, inexpensive, and biorenewable resource. In addition, the utilization of carbon dioxide either as a source of carbon or as a solvent is motivated in part by the health and safety benefits derived from its substitution for toxic chemicals.[2] Conforming with these objectives, the synthesis of polycarbonates *via* the alternative coupling of carbon dioxide and epoxides was first demonstrated by Inoue and co-workers in 1969.[3] Subsequent to Inoue's early discovery significant advances have been made from multinational research programs in the design of a wide variety of well-defined metal catalysts for this important transformation.[4] These studies have led to greatly improved catalytic activity, selectivity, and importantly a better understanding of the mechanistic aspects of this process for both *alicyclic* and *aliphatic* epoxide monomers. Nevertheless, the production of polycarbonates from aliphatic epoxides and CO_2 has suffered from the tendency of this coupling reaction to generally favor production of the corresponding five-membered cyclic carbonate.[5] This general propensity of aliphatic epoxides and CO_2 for selectively affording cyclic carbonates is somewhat unfortunate because their corresponding copolymers are biodegradable materials which possess a wide variety of potential applications, including those in biomedical areas such as drug delivery devices and tissue engineering applications.[6] Notwithstanding, recent ligand modifications have afforded catalyst systems with greatly enhanced selectivity for copolymer production from the coupling of propylene oxide and CO_2.[7] Hopefully, in the future these catalysts will be useful for copolymer synthesis from a wide variety of functionalized aliphatic epoxides.

An optional synthetic methodology for the production of aliphatic polycarbonates involves the ring-opening polymeri-

(1) (a) Aresta, M.; Dibenedetto, A. *Catal. Today* **2004**, *98*, 455–462. (b) Sakakura, T.; Choi, J.-C.; Yasuda, H. *Chem. Rev.* **2007**, *107*, 2365–2387. (c) Aresta, M.; Dibenedetto, A. *Dalton Trans.* **2007**, 2975–2992.

(2) Bottenbruch, L. *Engineering Thermoplastics: Polycarbonates, Polyacetals, Polyesters, Cellulose Esters*; Hanser Publishers: New York, 1996; p 112.

(3) Inoue, S.; Koinuma, H.; Tsuruta, T. *J. Polym. Sci., Part B: Polym. Phys.* **1969**, *7*, 287–292.

(4) (a) Chisholm, M. H.; Zhou, Z. *J. Mater. Chem.* **2004**, *14*, 3081–3092. (b) Darensbourg, D. J. *Chem. Rev.* **2007**, *107*, 2388–2410. (c) Darensbourg, D. J.; Holtcamp, M. W. *Coord. Chem. Rev.* **1996**, *153*, 155–174. (d) Darensbourg, D. J.; Mackiewicz, R. M.; Phelps, A. L.; Billodeaux, D. R. *Acc. Chem. Res.* **2004**, *37*, 836–844. (e) Kuran, W. *Prog. Polym. Sci.* **1998**, *23*, 919–992. (f) Moore, D. R.; Coates, G. W. *Angew. Chem., Int. Ed.* **2004**, *43*, 6618–6639. (g) Paddock, R. L.; Nguyen, S. T. *Macromolecules* **2005**, *38*, 6251–6253. (h) Sugimoto, H.; Inoue, S. *J. Polym. Sci., Part A: Polym. Chem.* **2004**, *42*, 5561–5573. (i) Super, M. S.; Beckman, E. J. *Trends Polym. Sci.* **1997**, *5*, 236–240. (j) Cohen, C. T.; Chu, T.; Coates, G. W. *J. Am. Chem. Soc.* **2005**, *127*, 10869–10878.

(5) (a) Kruper, W. J.; Dellar, D. V. *J. Org. Chem.* **1995**, *60*, 725–727. (b) Kuran, W.; Listos, T. *Macromol. Chem. Phys.* **1994**, *195*, 1011–1015.

(6) (a) Albertsson, A. C.; Eklund, M. *J. Polym. Sci., Part A: Polym. Chem.* **1994**, *32*, 265–279. (b) Pêgo, A. P.; Siebum, B.; VanLuyn, M. J. A.; Gellego, K. J.; Van Seijen, Y.; Poot, A. A.; Grijpma, D. W.; Feijen, J. *Tissue Eng.* **2003**, *9*, 981–994.

(7) (a) Nakano, K.; Kamada, T.; Nozaki, K. *Angew. Chem., Int. Ed.* **2006**, *45*, 7274–7277. (b) Noh, E. K.; Na, S. J.; Sujith, S.; Kim, S.-W.; Lee, B. Y. *J. Am. Chem. Soc.* **2007**, *129*, 8082–8083. (c) Cohen, C. T.; Coates, G. W. *J. Polym. Sci., Part A.: Polym. Chem.* **2006**, *44*, 5182–5191.

zation of six- and seven-membered cyclic carbonates. Unlike five-membered cyclic carbonates which are thermodynamically stable toward polycarbonate formation in the absence of CO_2 loss, six-membered cyclic carbonates can under certain catalytic conditions provide aliphatic polycarbonates with complete retention of their CO_2 contents (eq 1).[8] It is noteworthy that trimethylene carbonate is readily prepared from 1,3-propanediol and ethylchloroformate or diethylcarbonate.[9] Although, 1,3-propanediol is currently produced industrially from petroleum derivatives, in the context of sustainability it can also be synthesized by microbiological or biochemical routes.[10]

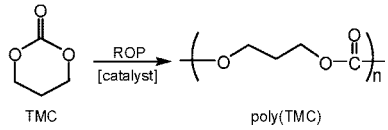

(1)

For the ring-opening polymerization (ROP) of trimethylene carbonate (TMC or 1,3-dioxan-2-one), salts of aluminum and tin have shown to be very effective catalysts.[11] Our group,[12] as well as Cao and co-workers,[13] has reported the use of effective salen complexes of aluminum as catalysts for this transformation. More recently, we also have shown the use of biometal derivatives as catalysts for the ring-opening polymerization of TMC and lactide.[14,15] The latter catalytic systems are of particular importance because the use of biocompatible metals, such as calcium, magnesium, and zinc, eliminates the difficulty of removing trace amounts of metal residues from the produced polycarbonates. Homoleptic lanthanide amidinate complexes,[16] samarium borohydride complexes,[17] and 2,2-dibutyl-2-stanna-1,3-oxepane[18] have also recently been investigated as catalysts for the ring-opening polymerization of trimethylene carbonate and its copolymerization with ε-caprolactone and L-lactide. In addition, organocatalysts in the presence of benzyl alcohol were reported by Hedrick as catalytic systems for the ROP of TMC, where high polymerization control, low polydispersities, and high end group fidelity could be obtained.[19] Similarly, Bowden and co-workers have utilized 2-(dimethylamino)ethanol as an effective catalyst for the ring-opening polymerization of TMC.[20]

Another alternative route to aliphatic polycarbonates involves the copolymerization of four-membered cyclic ethers, such as oxetane, and carbon dioxide (eq 2).

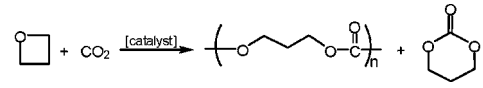

(2)

Surprisingly, this reaction has not been widely studied, but it is of particular interest, since in this case the cyclic carbonate byproduct, TMC, unlike five-membered cyclic carbonates, can be ring-opened and transformed into the alternating copolymer by means of the reaction defined in eq 1.

The first report on this reaction appeared in 1977 by Koinuma,[21] who employed a ternary catalytic system composed of triethylaluminium, water, and acetylacetone to copolymerize oxetane and carbon dioxide, producing poly(TMC) with a significant quantity of ether linkages. In this case, an anionic coordination mechanism was proposed for the formation of poly(TMC). Later, Matsuda[22] reported the use of organotin halide complexes in the presence of a base, to produce low molecular weight polycarbonates. Tetraphenylstibonium iodide was also employed by Matsuda to selectively synthesize trimethylene carbonate from oxetane and carbon dioxide.[23] In addition, Matsuda later on employed organotin iodide complexes with phosphines or phosphine oxides, to catalyze the addition of carbon dioxide to oxetane, yielding TMC and poly(TMC) products. It was demonstrated in this instance that the choice of the ligand was very important; all complexes with Bu_3P provided poly(TMC), but in the presence of $Bu_3P{=}O$, TMC was produced exclusively in good yields.[24] Moreover, Matsuda proposed a mechanism for the formation of poly(TMC), where TMC was formed first, and subsequent ring-opening polymerization of the preformed TMC produced poly(TMC).[24]

Of importance, these early reports on the coupling reaction of oxetane and carbon dioxide suggest that a full understanding of the mechanistic aspects of this process is lacking. Recently, our group has reported a variety of catalytic systems based on metal salen complexes for the copolymerization of cyclohexene oxide or propylene oxide and carbon dioxide.[4b] Optimizations of the catalytic systems and catalytic conditions have led us to produce copolymers with greater than 99% carbonate linkages, low polydispersities, and high molecular weights. This success has motivated us to examine the efficiency of metal salen complexes for the copolymerization reaction of oxetane and carbon dioxide to afford aliphatic polycarbonates. In a recent communication we presented preliminary studies on this reaction catalyzed by metal salen complexes of chromium and aluminum, where it was found that a (salen)-Cr(III)Cl complex (*N*,*N*′-bis(3,5-di-*tert*-butylsalicylidene)-1,2-ethylenediimine chromium(III) chloride) was more active than its aluminum salen analogue to catalyze this coupling reaction in the presence of *n*-Bu_4NN_3 as the cocatalyst.[25] In all the instances, high selectivity for copolymer formation was obtained even at high temperatures (110 °C). Based on circumstantial

(8) Clements, J. H. *Ind. Eng. Chem. Res.* **2003**, *42*, 663–674.
(9) (a) Ariga, T.; Takata, T.; Endo, T. *Macromolecules* **1997**, *30*, 737–744. (b) Carothes, W. H.; Natta, F. J. V. *J. Am. Chem. Soc.* **1930**, *52*, 314–326.
(10) (a) Tong, I. T.; Cameron, D. C. *Appl. Biochem. Biotechnol.* **1992**, *34/35*, 149–159. (b) Haynie, S.; Wagner, L.; Winona, L. (i.e. DuPont de Nemours and Co.)Patent WO/035799, 1996.
(11) Rokicki, G. *Prog. Polym. Sci.* **2000**, *25*, 259–342.
(12) Darensbourg, D. J.; Ganguly, P.; Billodeaux, D. R. *Macromolecules* **2005**, *38*, 5406–5410.
(13) Yang, J.; Yu, Y.; Li, Q.; Li, Y.; Cao, A. *J. Polym. Sci., Part A: Polym. Chem.* **2005**, *43*, 373–384.
(14) Darensbourg, D. J.; Choi, W.; Ganguly, P.; Richers, C. P. *Macromolecules* **2006**, *39*, 4374–4379.
(15) Darensbourg, D. J.; Choi, W.; Richers, C. P. *Macromolecules* **2007**, *40*, 3521–3523.
(16) Li, C.; Wang, Y.; Zhou, L.; Sun, H.; Shen, Q. *J. Appl. Polym. Sci.* **2006**, *102*, 22–28.
(17) Palard, I.; Schappacher, M.; Belloncle, B.; Soum, A.; Guillaume, S. M. *Chem.—Eur. J.* **2007**, *13*, 1511–1521.
(18) Pospiech, D.; Komber, H.; Jehnichen, D.; Häussler, L.; Eckstein, K.; Scheibner, H.; Janke, A.; Kricheldorf, H. R.; Petermann, O. *Biomacromolecules* **2005**, *6*, 439–446.
(19) Nederberg, F.; Lohmeijer, B. G. G.; Leibfarth, F.; Pratt, R. C.; Choi, J.; Dove, A. P.; Waymouth, R. M.; Hedrick, J. L. *Biomacromolecules* **2007**, *8*, 153–160.
(20) Mindemark, J.; Hilborn, J.; Bowden, T. *Macromolecules* **2007**, *40*, 3515–3517.
(21) Koinuma, H.; Hirai, H. *Makromol. Chem.* **1977**, *178*, 241–246.
(22) Baba, A.; Meishou, H.; Matsuda, H. *Makromol. Chem. Rapid Commun.* **1984**, *5*, 665–668.
(23) Baba, A.; Kashiwagi, H.; Matsuda, H. *Tetrahedron Lett.* **1985**, *26*, 1323–1324.
(24) Baba, A.; Kashiwagi, H.; Matsuda, H. *Organometallics* **1987**, *6*, 137–140.
(25) Darensbourg, D. J.; Ganguly, P.; Choi, W. *Inorg. Chem.* **2006**, *45*, 3831–3833.

evidence, it was suggested that formation of copolymer did not proceed *via* the intermediacy of TMC which was observed as a minor product of the coupling reaction.

Herein, we have extended these investigations by further optimizing the (salen)CrCl catalytic system for this reaction. Efforts have been made to gain a greater insight into the mechanistic aspects of this important reaction based on kinetic and copolymer end-group analysis studies performed utilizing *in situ* infrared and ^{1}H NMR spectroscopies.

Experimental Section

Reagents and Methods. Unless otherwise specified, all syntheses and manipulations were carried out on a double-manifold Schlenk vacuum line under an atmosphere of argon or in an argon filled glovebox. Toluene and tetrahydrofuran were freshly distilled from sodium/benzophenone. Ethanol was freshly distilled from Mg/I_2. 1,1,2,2-tetrachloroethane (TCE) was freshly distilled from CaH_2. Diethyl ether, dichloromethane, and pentane were purified by an MBraun Manual Solvent Purification System packed with Alcoa F200 activated alumina desiccant. Oxetane (Alfa Aesar) was freshly distilled from CaH_2 and stored in the freezer of the glovebox. Trimethylene carbonate (Boehringer Ingelheim) was recrystallized from tetrahydrofuran and diethyl ether, dried under vacuo, and stored in the glovebox. Tricyclohexylphosphine (Alfa Aesar) was recrystallized from distilled ethanol before use. PPNCl ($PPN^+ = (Ph_3P)_2N^+$) (Aldrich) was recrystallized from dichloromethane/ether before use, and $PPNN_3$ was synthesized according to a published procedure.[26] Tetra-*n*-butylammonium bromide (Aldrich) was recrystallized from acetone/diethyl ether before use. Tetra-*n*-butylammonium azide (TCI) was stored in the freezer of the glovebox upon arrival. Bone-dry carbon dioxide supplied in a high-pressure cylinder and equipped with a liquid dip tube was purchased from Scott Specialty Gases. The corresponding salen ligands and chromium complexes were synthesized as previously described.[27]

^{1}H NMR spectra were acquired on Unity+ 300 MHz and VXR 300 MHz superconducting NMR spectrometers. IR spectra were recorded on a Mattson 6021 Fourier Transform (FT) IR spectrometer with an MCT detector. TGA measurements were performed with SDT Q600 V7.0 Build 84. Analytical elemental analysis was provided by Canadian Microanalytical Services Ltd. Molecular weight determinations (M_n and M_w) were carried out with a Viscotek Modular GPC apparatus equipped with ViscoGEL I-series columns (H + L) and a model 270 dual detector comprised of refractive index and light scattering detectors. High-pressure reaction kinetic measurements were performed using an ASI ReactIR 1000 reaction analysis system with a stainless steel Parr autoclave modified with a permanently mounted ATR crystal (SiComp) at the bottom of the reactor (purchased from Mettler Toledo).

Results and Discussion

Initially we chose to employ the (salen)CrCl catalyst, complex **1** in Figure 1, in the presence of various cocatalysts to optimize the selectivity for copolymer formation from the coupling of oxetane and carbon dioxide. The copolymerization reactions were performed under identical reaction conditions, i.e., 110 °C and 35 bar CO_2 pressure. The results are summarized in Table 1, where the counterions of the anionic initiators were either $PPN^+[(Ph_3P)_2N^+]$ or *n*-Bu_4N^+. The product mixtures were analyzed by ^{1}H NMR spectroscopy, with the quantities of poly(TMC), TMC, and ether linkages in the poly(TMC) determined by integrating the resonances at 4.23, 4.43, and 3.50 ppm, respectively. As is readily seen in Table 1, the yield of poly(TMC) is much greater than that of the cyclic product, TMC, at the end of a 24 h reaction period in all instances. Of importance here, the azide salts are slightly better than their chloride analogues, with little difference between the PPN^+ and *n*-Bu_4N^+ salts being observed. The bromide anion was shown to be significantly less selective for copolymer formation than the chloride anion, and tricyclohexylphosphine displayed the lowest selectivity toward copolymer formation of the cocatalysts studied.[28]

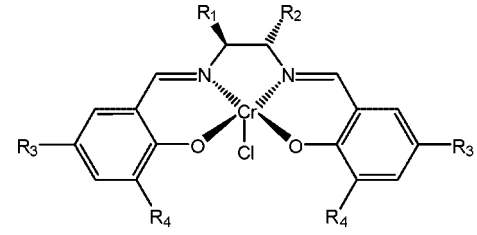

Complex **1**: $R_1 = R_2 = H$; $R_3 = R_4 = t$-Bu
2: $R_1, R_2 = -C_4H_4-$; $R_3 = R_4 = t$-Bu
3: $R_1, R_2 = -C_4H_4-$; $R_3 = OMe$; $R_4 = t$-Bu
4: $R_1, R_2 = (1R,2R)$-C_4H_8- ; $R_3 = R_4 = t$-Bu

Figure 1. Structures of the (salen)Cr(III) chloride complexes utilized as catalysts for the copolymerization of oxetane and CO_2.

Table 1. Selectivity for Copolymer Formation using Complex **1** in the Presence of Various Cocatalysts[a]

entry	cocatalyst	% TMC[b]	% poly(TMC)[b]	% ether linkages[b]
1	*n*-Bu_4NCl[c]	0	100	3.0
2	*n*-Bu_4NN_3[c]	0	100	2.9
3	*n*-Bu_4NBr	11.7	88.2	7.2
4	PPNCl	5.9	94	3.6
5	$PPNN_3$	2.3	97.6	1.4
6	$P(Cy)_3$	21.1	79	21.5

[a] Copolymerization conditions: 17 mg of catalyst (0.15 mol%), 1.15 g of oxetane, M/I = 675:1, 2 equiv of cocatalyst, 10 mL of toluene, 35 bar of CO_2, at 110 °C for 24 h. [b] Product distributions were determined by ^{1}H NMR spectroscopy. [c] Previous published results.[25] Note for the first entry in Table 1 in ref 25, the % TMC is incorrectly reported due to misassigned ^{1}H NMR resonances.

Subsequent studies were carried out to interrogate the effects of changing the nature of (i) the substituents on the phenolate rings and (ii) the diimine backbone of the salen ligand in the (salen)CrCl derivative. In this instance the copolymerization reactions were performed at a monomer/catalyst/cocatalyst ratio of 1292:1:2, with a CO_2 pressure of 35 bar at 110 °C for 24 h. The results of this inquiry are provided in Table 2, where the TOFs (mol of oxetane consumed/mol of initiator·h) were determined from the *isolated copolymer* obtained upon precipitation from dichloromethane with a 1 M HCl solution in methanol. It is important to note here that minimal quantities of ether linkages were observed in the copolymer samples resulting from consecutive oxetane ring-opening processes; however, in all cases the CO_2 content was very high (>95%). Note that 100% carbon dioxide incorporation defines a *completely alternating* copolymer of oxetane and CO_2. The molecular weights of the copolymers were determined in THF solution by gel permeation chromatography using RI and light scattering detectors and polystyrene standards. In general, the observed

(26) Demadis, K. D.; Meyer, T. J.; White, P. S. *Inorg. Chem.* **1998**, *37*, 3610–3619.
(27) Darensbourg, D. J.; Mackiewicz, R. M.; Rodgers, J. L.; Fang, C. C.; Billodeaux, D. R.; Reibenspies, J. H. *Inorg. Chem.* **2004**, *43*, 6024–6034.
(28) (a) Darensbourg, D. J.; Mackiewicz, R. M. *J. Am. Chem. Soc.* **2005**, *127*, 14026–14038. (b) Darensbourg, D. J.; Mackiewicz, R. M.; Rodgers, J. R. *J. Am. Chem. Soc.* **2005**, *127*, 17565.

Table 2. Copolymerization of Oxetane and CO_2 Catalyzed by (salen)Cr(III)Cl Complexes[a]

entry	complex	R_1	R_2	R_3	R_4	TON[b]	TOF[c]	% CO_2 content[d]	% conversion[d]
1	**2**	$-C_4H_4-$		*tert*-butyl	*tert*-butyl	588	24.5	97.1	54.6
2	**3**	$-C_4H_4-$		OCH_3	*tert*-butyl	382	15.9	97.5	33.3
3	**1**	H	H	*tert*-butyl	*tert*-butyl	775	32.3	95.5	67.9
4	**4**	(1*R*,2*R*)-C_4H_8-		*tert*-butyl	*tert*-butyl	835	34.8	95.9	71.6

[a] Copolymerization conditions: Catalyst loading = 0.077 mol %, 4 g of oxetane, 2 equiv of *n*-Bu_4NN_3, M/I = 1292, 35 bar of CO_2, at 110 °C for 24 h. [b] Mol of oxetane consumed/mol of initiator. [c] Mol of oxetane consumed/(mol of initiator·h). [d] Estimated by ^{1}H NMR spectroscopy.

Table 3. Molecular Weights and Polydispersities of Poly(TMC)[a]

entry	M/I	% conversion[b]	M_n (GPC)	M_n (theoretical)[c]	M_w/M_n(GPC)
1	150	99.5	11 200	15 200	1.26
2	275	90.7	9500	25 500	1.45
3	350	48.5	6700	17 300	1.43
4	475	29.7	7050	14 400	1.60
5[d]	150	100.0	14 500	15 300	1.30

[a] Copolymerization conditions: Reactions carried out in toluene at 110 °C using (salen)Cr(III)Cl catalyst, 2 equiv of *n*-Bu_4NN_3 as cocatalyst at 35 bar CO_2 pressure. [b] Estimated by ^{1}H NMR spectroscopy. [c] M_n(theoretical) = M/I × mol wt(oxetane + CO_2) × % conversion. [d] Done in the absence of solvent using $PPNN_3$ as cocatalyst.

Scheme 1

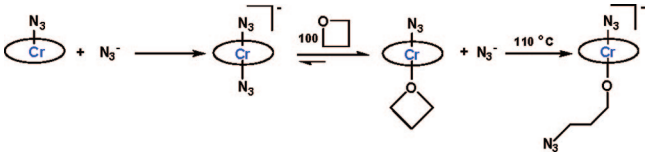

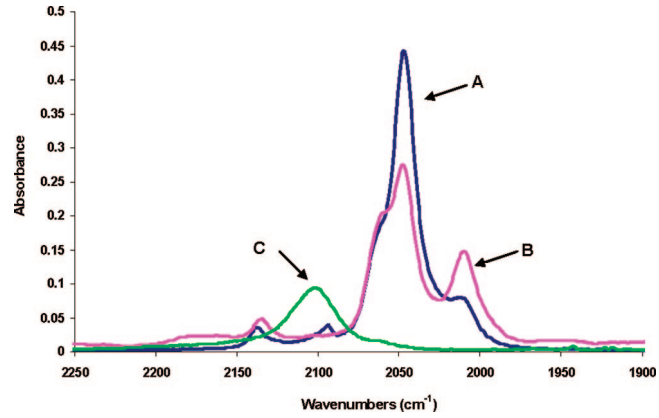

Figure 2. Spectra of TCE solutions of chromium salen azide complex with 1 equiv of *n*-Bu_4NN_3(A), after addition of 100 equiv of oxetane at room temperature (B), after heating the reaction solution at 110 °C for 3 h (C).

M_n values were found to be much lower than the theoretical values; e.g., in entry 4 of Table 2 the observed M_n 11 050 is considerably lower than the theoretical value 85 000. This is most likely due to a chain transfer mechanism arising from the presence of trace quantities of water in the system.[7a,29] The PDI was in general about 1.5, and a copolymer with an M_n of 11 050 was found to be stable up to 260 °C by TGA. A more comprehensive compilation of molecular weights as a function of the monomer/initiator ratio, along with polydispersities, can be found in Table 3. Included in Table 3 is a catalytic run done under superanhydrous conditions, i.e., no solvent and in the presence of the less hydroscopic $PPNN_3$ salt. As is evident under these conditions the molecular weight more closely tracks the predicted value.

Retaining the salen ligand with the phenylene backbone while changing the substituents in the 3,5-positions of the phenolate rings (entries 1 and 2, Table 2) reveals the Cr(III) salen derivative containing the bulky di-*tert*-butyl groups to be the more active. This is consistent with previous observations reported for the ROP of TMC catalyzed by aluminum and calcium salen complexes.[12,14,15] On the other hand, for the copolymerization of cyclohexene oxide and CO_2 catalyzed by chromium salen complexes, higher catalytic activity was obtained in complexes containing methoxy and *tert*-butyl groups in the 3- and 5-positions of the phenolate rings.[27] We have also studied the effects of altering the diimine backbone of the Cr(III) salen complex while maintaining the di-*tert*-butyl groups in the 3,5-positions of the phenolate moiety (entries 3 and 4, Table 2). As can be seen in Table 2, the catalytic behavior of the chromium salen complexes is not much affected by changing the diimine backbone from ethylene to cyclohexylene, with the chromium salen complex with the cyclohexylene backbone displaying slightly higher catalytic activity.

Substrate Binding and Ring-Opening Steps Examined by Infrared Spectroscopy. Fundamental to a better understanding of the mechanism of the coupling reaction of oxetane and carbon dioxide is an investigation of the initiation step of this process. Since it is known that oxetane has less ring strain compared to epoxides, e.g., the heat of polymerization of ethylene oxide ($-\Delta H_p$ = 104 kJ/mol) differing from that of oxetane by 23 kJ/mol,[30] its ease of ring opening should depart significantly from that of epoxides. In order to address this issue we have conducted cocatalyst, oxetane binding, and subsequent ring-opening studies *via* infrared spectroscopy using the (salen)CrN_3 complex containing di-*tert*-butyl substituents in the 3,5-positions of the phenolate rings and an ethylene backbone for the diimine. We have employed the azide derivatives for these studies because the ν_{N_3} stretching vibration provides accessible probes for both cocatalyst binding and anion ring-opening steps. The results of these studies are depicted in Scheme 1 and Figure 2.

As indicated in Scheme 1, upon addition of 1 equiv of *n*-Bu_4NN_3 to (salen)CrN_3, the anionic six-coordinate *bis*-azide species (salen)$Cr(N_3)_2^-$ readily forms at ambient temperature. This is apparent in the ν_{N_3} stretching region where the infrared band of (salen)CrN_3 shifts from 2083 cm^{-1} to a band at 2047 cm^{-1} with a shoulder at 2057 cm^{-1} upon addition of *n*-Bu_4NN_3. It should be noted here that the *n*-Bu_4N^+ salts of numerous (salen)CrX_2^- anions have been fully characterized by X-ray crystallography and these studies will be reported elsewhere. For example, Figure 3 illustrates the solid-state structure of the *bis*-azide anion of one such derivative. Addition of a 100-fold excess of oxetane to the *bis*-azide complexes displaces some

(29) (a) Darensbourg, D. J.; Fitch, S. B. *Inorg. Chem.* **2007**, *47*, 5474–5476. (b) Sugimoto, H.; Ohtsuka, H.; Inoue, S. *J. Polym. Sci., Part A: Polym. Chem.* **2005**, *43*, 4172–4186.

(30) Sawada, H. *Macromol. Sci., Rev. Macromol. Chem.* **1970**, *C5*, 151–174.

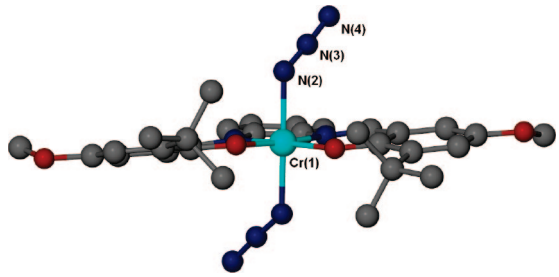

Figure 3. Ball-and-stick representation of the X-ray defined structure of the anion of the [*n*-Bu_4N][(salen)$Cr(N_3)_2$] complex, where the salen ligand contains −OMe and ^{t}Bu substituents in the 3,5-positions of the phenolates, respectively, with a phenylene diimine backbone.

of the azide ligand as can be seen by an increase in the free azide ion concentration by its ν_{N_3} band at 2009 cm^{-1} with a concomitant decrease in the concentration of (salen)$Cr(N_3)_2^-$ (spectrum B). Moreover, a new ν_{N_3} stretching band appears at 2061 cm^{-1} which is assigned to (salen)$Cr(N_3)$·oxetane. Upon stirring this reaction mixture for 24 h at ambient temperature no changes in the infrared spectrum resulted, indicative of the ring-opening process of oxetane requiring higher temperatures. Indeed, heating the reaction mixture for 3 h at 110 °C led to oxetane ring opening by azide as indicated by the organic azide band at 2100 cm^{-1}. It should be recalled that an analogous experiment carried out with cyclohexene oxide results in epoxide ring-opening by azide at ambient temperature, although the equilibrium between (salen)$Cr(N_3)_2^-$ and cyclohexene oxide lies much farther to the left.[27] That is, cyclohexene oxide has less of a penchant for displacing the azide from the chromium(III) center than the more basic oxetane monomer.

X-ray crystallography was utilized in conjunction with the ν_{N_3} infrared spectral data (*vide supra*) to verify that oxetane binding to the chromium center occurs without ring-opening at ambient temperature. Two (salen)CrCl complexes with oxetane bound to the chromium centers were successfully characterized by X-ray crystallography. To the best of our knowledge these represent the only crystal structures of oxetane bound to a metal center thus far reported in the literature. Crystallographic data pertaining to these two crystal structures are provided in Table 4.

In our first attempt at isolating single crystals of a (salen)CrCl complex with an axially coordinated oxetane, the presence of trace quantities of water led to hydrolysis of the Cr−Cl bond. Nevertheless, crystals of a hydroxo-bridged structure with oxetane bound to one of the chromium centers were obtained which were suitable for X-ray analysis (Figure 4 and Table 5). Similar solid-state structures of hydroxo-bridged chromium(III) derivatives have been reported by us resulting from the complete hydrolysis of (acacen)CrCl or (salen)CrOMe derivatives.[31] Complex **5** clearly shows that oxetane is capable of binding to the (salen)Cr(III) center without undergoing ring-opening at ambient temperature. The oxetane molecule is disordered in complex **5**. Upon modeling the disorder two different positions for the oxetane ligand were found, where the dihedral angles of the plane C−O−C and C−C−C were determined to be 4.5° and 10.8° at 110 K. That is, the oxetane molecule is not planar, which is in good agreement with the structure of free oxetane reported by Luger and Buschmann where the dihedral angle was found to be 10.7° at 90 K and 8.7° at 140 K.[32]

A successful isolation of single crystals of an oxetane adduct as depicted in Scheme 1 was achieved upon utilizing superdry conditions and low temperature. Complex **6** was fully characterized by X-ray crystallography, and a thermal ellipsoid representation of this derivative is shown in Figure 5, with selected

Table 4. Crystallographic Data for Complexes **5** and **6**

	5	**6**
empirical formula	$C_{80}H_{110}ClCr_2N_4O_6$	$C_{34.40}H_{48.80}Cl_{3.20}Cr_{0.80}N_{1.60}O_{2.40}$
fw	1364.17	678.19
temperature (K)	110(2)	110(2)
crystal system	triclinic	triclinic
space group	$P\bar{1}$	$P\bar{1}$
a (Å)	12.266(5)	16.175(5)
b (Å)	14.702(5)	16.394(5)
c (Å)	21.630(5)	17.126(5)
α (deg)	102.839(5)	89.781(4)
β (deg)	95.784(5)	88.053(4)
γ (deg)	100.245(5)	79.249(4)
V (Å^3)	3702(2)	4459(2)
D_c (Mg/m^3)	1.223	1.263
Z	2	5
abs coeff (mm^{-1})	0.384	0.535
reflections collected	10 087	41 341
independent reflections	10 392 [(int) = 0.0755]	15 610 [R(int) = 0.0612]
restrains/parameters	51/856	48/979
GOF on F^2	1.029	1.077
final R indices [$I > 2\sigma(I)$]	$^aR_1 = 0.0755$ $^bR_w = 0.1995$	$^aR_1 = 0.0579$ $^bR_w = 0.1433$
final R indices (all data)	$^aR_1 = 0.1239$ $^bR_w = 0.2321$	$^aR_1 = 0.0908$ $^bR_w = 0.1643$

^{a} $R = \Sigma||F_o| - |F_c||/\Sigma|F_o|$. ^{b} $R_w = \{[\Sigma w(F_o^2 - F_c^2)^2]/[\Sigma w(F_o^2)^2]\}^{1/2}$; $w = 1/[\sigma^2(F_o^2) + (aP)^2 + bP]$, where $P = [(\max(F_o^2), 0) + 2(F_c^2)]/3$.

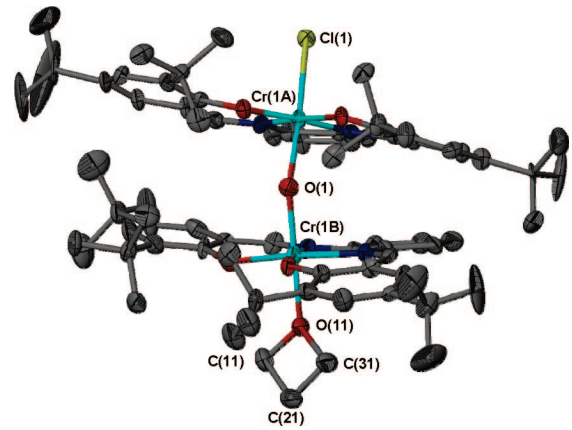

Figure 4. Thermal ellipsoid plot of complex **5**. Ellipsoids are at the 50% level. H atoms are omitted for clarity. One pentane molecule was crystallized in the unit cell and is omitted for clarity.

Table 5. Selected Bond Distances and Angles for Complex **5**^{a}

Cr(1A)−Cl(1)	2.342(3)
Cr(1A)−O(1)	2.007(6)
Cr(1B)−O(1)	1.949(6)
Cr(1B)−O(11)	2.054(9)
O(11)−C(11)−C(21)	90.5(8)
O(11)−C(31)−C(21)	90.5(8)
C(11)−O(11)−C(31)	91.1(7)
C(31)−C(21)−C(11)	87.6(8)

^{a} Units of bond angles and bond distances are (deg) and (Å), respectively.

(31) Darensbourg, D. J.; Frantz, E. B.; Andreatta, J. R. *Inorg. Chim. Acta* **2007**, *360*, 523–528.
(32) Luger, P.; Buschmann, J. *J. Am. Chem. Soc.* **1984**, *106*, 7118–7121.

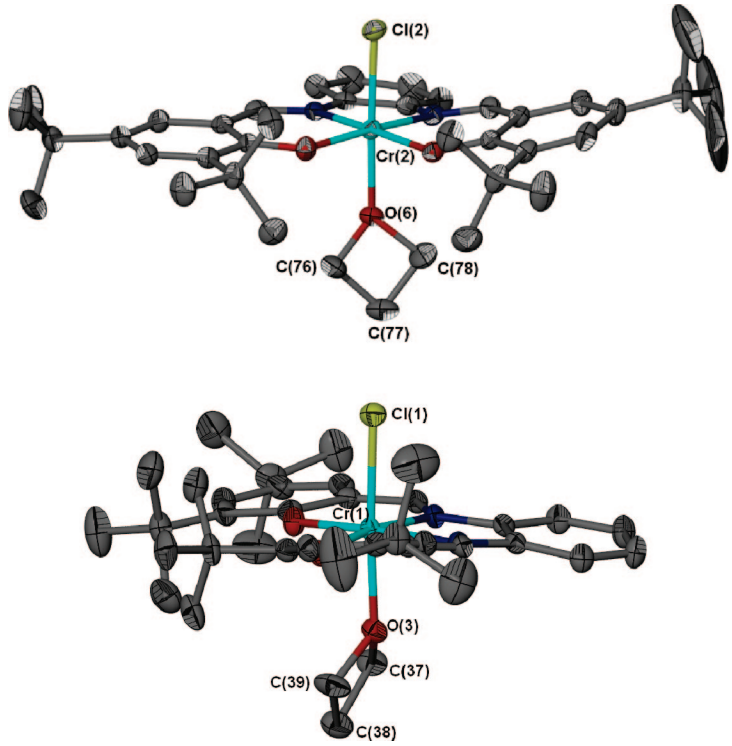

Figure 5. Thermal ellipsoid plot of complex **6**. Ellipsoids are at the 50% level. H atoms are omitted for clarity. Three dichloromethane and one pentane molecules were crystallized in the unit cell and are omitted for clarity.

Table 6. Selected Bond Distances and Angles for Complex **6**[a]

Cr(1)−Cl(1)	2.3167(6)
Cr(2)−Cl(2)	2.3036(7)
Cr(1)−O(3)	2.0456(10)
Cr(2)−O(6)	2.0528(11)
O(6)−C(76)−C(77)	90.75(11)
O(6)−C(78)−C(77)	90.88(12)
C(78)−C(77)−C(76)	85.72(12)
C(78)−O(6)−C(76)	90.08(11)

[a] Units for bond distances and bond angles are (Å) and (deg), respectively.

bond distances and bond angles listed in Table 6. Two molecules crystallized in the asymmetric unit, where the sum of the angles in the oxetane ligands is 359.6° and 357.4°, respectively. The dihedral angles of the planes C−O−C and C−C−C in the oxetane ligands were found to be 10.5° and 11.8° at 110 K, which clearly demonstrates that the oxetane molecule when bound to the metal center maintains its degree of nonplanarity. Metric parameters for free oxetane and bound oxetane in complex **6** are quite comparable as seen in Table 7.

Kinetic Studies of the Copolymerization of Oxetane and Carbon Dioxide. Kinetic measurements of the coupling reaction of oxetane and carbon dioxide were performed in toluene solution in the presence of complex **4** along with 2 equiv of *n*-Bu_4NN_3. These reactions were monitored by *in situ* infrared spectroscopy by observing the growth of the copolymer's $\nu_{C=O}$ band at 1750 cm^{-1} as a function of time. A typical reaction profile of the absorbance of the 1750 cm^{-1} infrared band with time is illustrated in Figure 6. It should be noted as well in Figure 6 that at the early stages of the coupling reaction a $\nu_{C=O}$ band at ∼1770 cm^{-1} assigned to TMC was observed which subsequently disappeared. Furthermore, the presence of the induction period seen in Figure 6 can be attributed to the drop in temperature of ∼20 °C observed following the addition of carbon dioxide to the 110 °C reaction mixture, as well as a slow initiation step.

The copolymerization reactions were demonstrated to be first-order in oxetane and catalyst (complex **4**) concentrations in the presence of 2 equiv of *n*-Bu_4NN_3. This is shown in a representative case in Figure 7 where a plot of $\ln[(A_\infty - A_t)/(A_\infty - A_o)]$ vs time for the formation of copolymer is found to be linear, with A_∞ and A_t being the absorbance of the $\nu_{C=O}$ band of the copolymer at $t = \infty$ and $t =$ time, respectively. It is important to note here that the data plotted in Figure 7 are for the early portion of the reaction because at higher levels of conversion (>65%) the reaction solution becomes more viscous.[29] Similarly, the order of the reaction with regard to complex **4** was observed to be first-order based on the linear relationship between initial rate vs complex **4** concentration (Figure 8). As is readily seen in Figure 8, the linear plot has a nonzero intercept of the *x*-axis of ∼0.005 M, suggesting that a small quantity of the catalyst is degraded in the copolymerization process. Relevant to this latter point, when the copolymerization reaction is carried out under identical conditions except in neat oxetane at a catalyst concentration of 0.005 M the system is active for copolymer formation.

The dependence of the coupling of oxetane and carbon dioxide on the concentration of the anionic initiator (cocatalyst) was examined in the instance of *n*-Bu_4NN_3. As is evident in Figure 9 the copolymerization rate was found to be first-order in [cocatalyst] up to approximately 2 equiv of *n*-Bu_4NN_3. Hence, in the range of [*n*-Bu_4NN_3] investigated between 0.5 and 2.0 equiv, the copolymerization process can be described as being first-order in oxetane, (salen)CrX, and cocatalyst concentrations, with zero-order dependence on [cocatalyst] greater than 8–10 equiv. This latter behavior is to be expected for a reaction where the initiation step is not significantly faster than the propagation step.

Table 7. Selected Bond Distances and Angles for Oxetane Molecules[a]

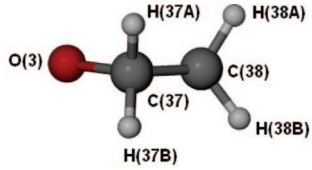

Oxetane molecule(1) from complex **6**.

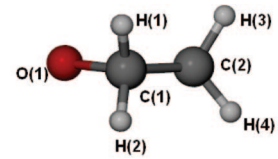

Free oxetane molecule from reference (32).

C(39)-O(3)	1.458(17)	O(3)-C(37)-C(38)	90.54(11)	C(1)-O(1)	1.433(2)	O(1)-C(1)-C(2)	91.89(9)
C(37)-O(3)	1.482(18)	O(3)-C(39)-C(38)	91.55(11)	C(3)-O(1)	1.433(2)	O(1)-C(3)-C(2)	91.89(9)
C(37)-C(38)	1.516(2)	C(39)-O(3)-C(37)	90.13(10)	C(1)-C(2)	1.517(2)	C(1)-O(1)-C(3)	90.5(1)
C(38)-C(39)	1.514(2)	C(39)-C(38)-C(37)	86.79(11)	C(2)-C(3)	1.517(2)	C(1)-C(2)-C(3)	85.0(1)
C(37)-H(37B)	0.99			C(1)-H(2)	0.99(2)		
C(38)-H(38B)	0.99			C(2)-H(4)	0.97(3)		
Dihedral angle of the plane C-O-C and C-C-C: 10.5				Dihedral angle of the plane C-O-C and C-C-C: 10.7			

[a] Units for bond distances and bond angles are (Å) and (deg), respectively.

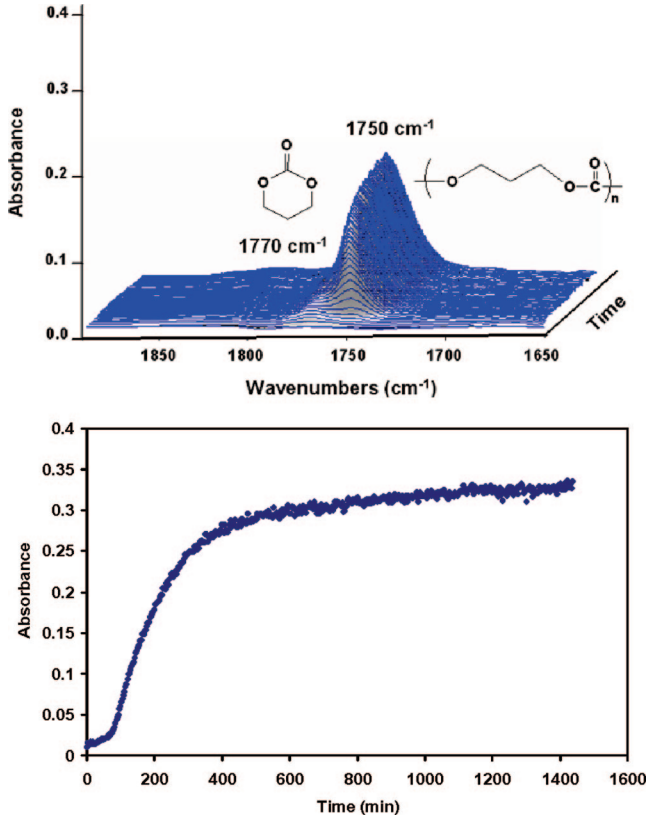

Figure 6. Three-dimensional stack plot reaction profile of the IR spectra collected every 3 min during the copolymerization reaction of oxetane and carbon dioxide. Reaction carried out at 110 °C in toluene at 35 bar CO_2 pressure.

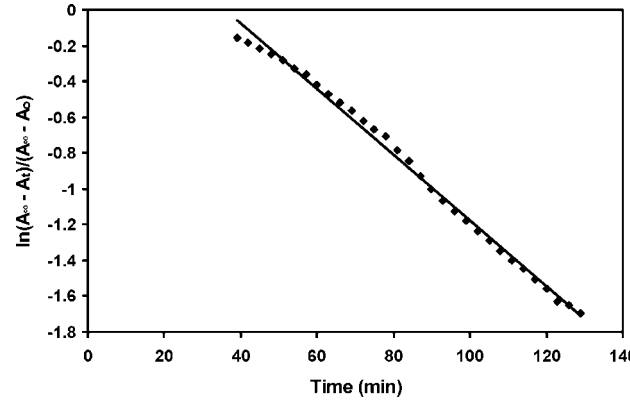

Figure 7. First-order plot of the conversion of oxetane and CO_2 to poly(TMC). Reaction carried out in toluene at 110 °C with complex **4** (0.0327 M), 2 equiv of n-Bu_4NN_3 at 35 bar CO_2 pressure. Oxetane concentration = 4.92 M. Slope = −0.0183, y intercept = 0.6525 with R^2 = 0.9946.

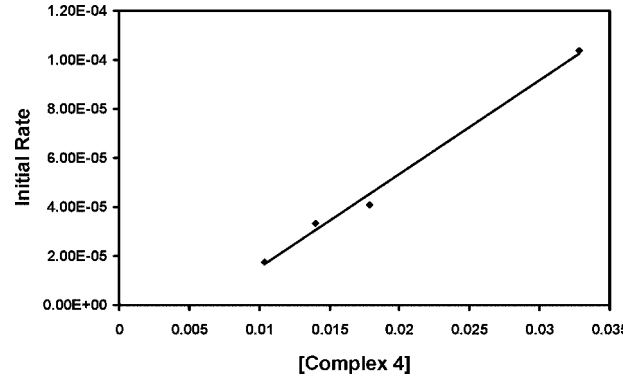

Figure 8. Dependence of copolymerization reaction on [catalyst]. Reactions carried out in toluene at 110 °C with complex **4**, 2 equiv of n-Bu_4NN_3 at 35 bar CO_2 pressure. Oxetane concentration = 4.92 M. Initial rate vs [complex **4**] provided a y-intercept of -2.10^{-5} with R^2 = 0.9931.

The copolymerization of oxetane and CO_2 was performed at several temperatures between 80 and 110 °C, and the observed rate constants for the process k_p, where rate = k_p[oxetane][catalyst][cocatalyst], were determined. These k_p values as a function of temperature are listed in Table 8, with the corresponding Eyring plot depicted in Figure 10. The calculated activation parameters $\Delta H^{\ddagger}$ and $\Delta S^{\ddagger}$ were 45.6 ± 3 kJ/mol and −161.9 ± 8.2 J/mol·deg, respectively. In this instance the enthalpy of activation ($\Delta H^{\ddagger}$) is very similar to that observed for the copolymerization of cyclohexene oxide and CO_2 (45.5 kJ/mol)

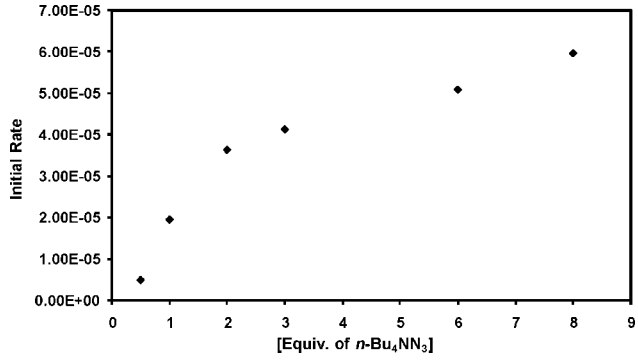

Figure 9. Initial rates for production of poly(TMC) as a function of number of equivalents of cocatalyst. Reactions carried out in toluene at 110 °C with complex **4** (0.014 M) and *n*-Bu_4NN_3 as cocatalyst, at 35 bar CO_2 pressure, oxetane concentration = 4.92 M.

Table 8. Variable Temperature Rate Constants for the Copolymerization Reaction[a]

T (K)	k_p ($L^2/mol^2 \cdot s$)
353	0.00449
363	0.00741
373	0.0103
383	0.0171

[a] Each experiment was performed in toluene at 110 °C with 0.014 M of complex **4** and 2 equivalents of *n*-Bu_4NN_3 at 35 bar CO_2 pressure. Oxetane concentration = 4.92 M.

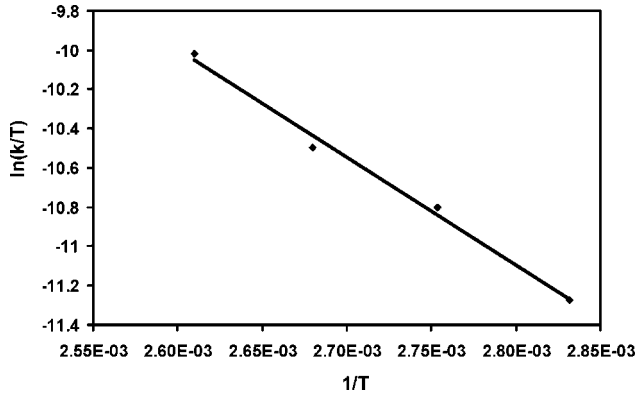

Figure 10. Eyring plot for the formation of poly(TMC) in the presence of complex **4**/*n*-Bu_4NN_3 catalyst system in toluene. Slope = −5502.5 with $R^2 = 0.992$.

and lower than that for the process involving the monomers propylene oxide and CO_2 (66.2 kJ/mol) employing a similar catalyst system.[33,34]

Solution Kinetic Studies of the Ring-Opening Polymerization of Trimethylene Carbonate. Herein we wish to describe in detail kinetic measurements for the ring-opening polymerization of trimethylene carbonate to poly(TMC), eq 1, under comparable conditions to that reported above for the copolymerization of oxetane and CO_2 leading to poly(TMC).[35] In this instance the use of 1,1,2,2-tetrachloroethane was found to be advantageous because of its high boiling point and the high solubility of both monomer and polymer in a chlorinated solvent. These reactions

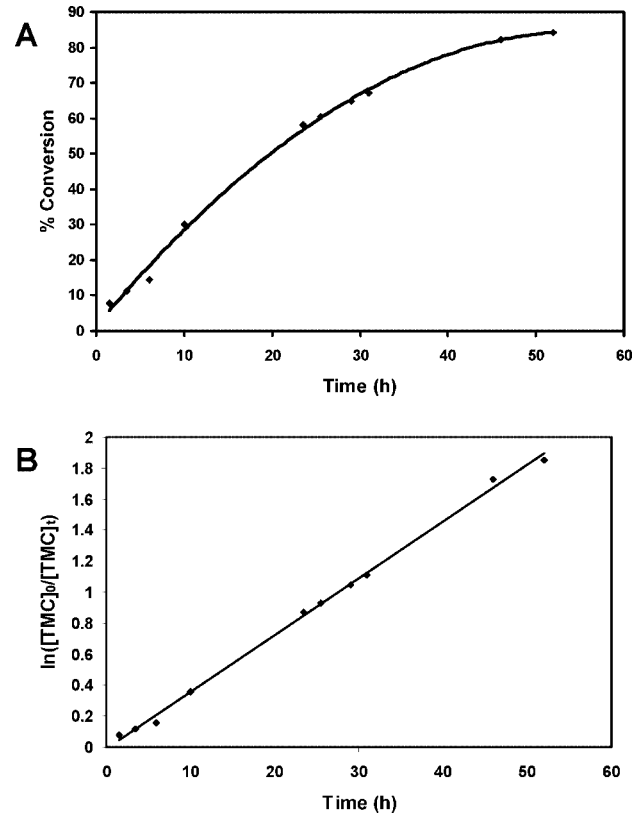

Figure 11. (A) Plot of monomer conversion vs time. (B) First-order plot of the conversion of TMC to poly(TMC). Reaction carried out in TCE at 120 °C with complex **4** (0.005 06 M) and 2 equiv of *n*-Bu_4NN_3 (0.0098 M). TMC concentration = 0.98 M, Slope = 0.0366, *y*-intercept = −0.0092 with $R^2 = 0.9975$.

Table 9. Rate Constant Dependence on the Concentrations of Catalyst and Cocatalyst for the ROP of TMC[a]

entry	[catalyst] (mol/L)	equiv of *n*-Bu_4NN_3	temp (°C)	k_{obsd} (h^{-1})
1	0.002 53	2	120	0.0169
2	0.003 80	2	120	0.0295
3	0.005 06	2	120	0.0366
4	0.010 10	2	120	0.071
5	0.005 06	0	120	0.0055
6	0.005 06	0.5	120	0.0168
7	0.005 06	0.75	120	0.0225
8	0.005 06	1	120	0.0275
9	0.005 06	2	120	0.0366
11	0.005 06	3	120	0.0414
12	0.005 06	6	120	0.0473
13	0.005 06	8	120	0.0530

[a] Monomer concentration held at 0.98 M. Reactions carried out in 1,1,2,2,-tetrachloroethane at atmospheric pressure.

were monitored by ^1H NMR spectroscopy. Figure 11a displays a typical monomer consumption vs time plot, whereas the semilogarithmic plot of $-\ln([monomer]_0/[monomer]_t)$ vs time is displayed in Figure 11b, and as might be expected the polymerization reaction was found to be first-order with respect to [TMC]. Table 9 summarizes the determined rate constants for the ROP of TMC as a function of [catalyst] and [cocatalyst]. Log–log plots of the rate constants vs [catalyst] and [cocatalyst] reveal relationships between ln k_{obsd} vs ln[catalyst] or ln[cocatalyst] with slopes close to unity, thus, indicative of the polymerization reaction being first-order in [catalyst] and first-order with respect to [cocatalyst] up to 1 equiv of cocatalyst.

Figures 12 and 13 illustrate the effect of excess quantities of cocatalyst (*n*-Bu_4NN_3) on the rate constant of the ring-opening

(33) Darensbourg, D. J.; Yarbrough, J. C. *J. Am. Chem. Soc.* **2002**, *124*, 6335–6342.
(34) Darensbourg, D. J.; Yarbrough, J. C.; Ortiz, C.; Fang, C. C. *J. Am. Chem. Soc.* **2003**, *125*, 7586–7591.
(35) We have previously described the ROP of TMC catalyzed by complexes dervied from biocompatible metals.[12,14,15]

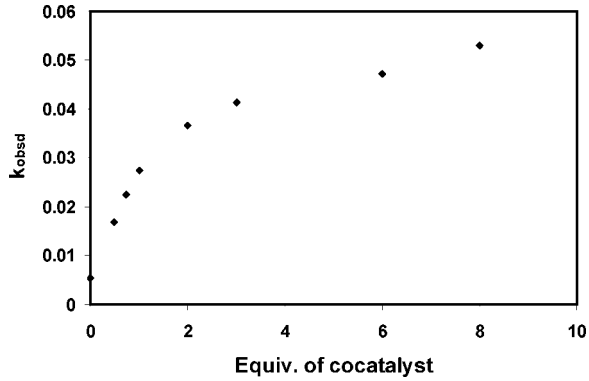

Figure 12. Rate constant for production of poly(TMC) as a function of number of equivalents of cocatalyst (n-Bu_4NN_3). Data taken from Table 8.

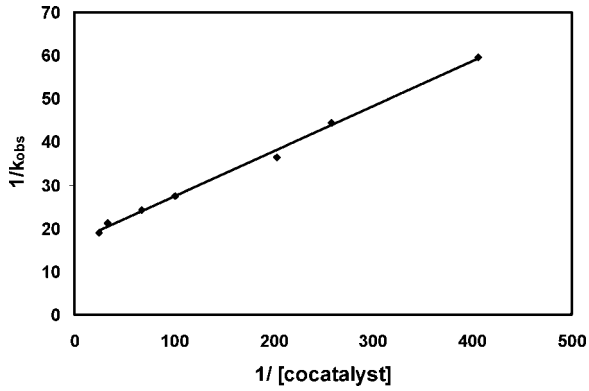

Figure 13. Double reciprocal plot of the rate constant dependence of the ROP process with [cocatalyst]. Data taken from Table 8. Slope = 0.1044 and y-intercept = 16.792 with $R^2 = 0.9966$.

Table 10. Variable Temperature Rate Constants for the Polymerization Reaction[a]

T (K)	k_p ($L^2/mol^2 \cdot s$)
378	0.07621
383	0.10469
393	0.19854
403	0.34825

[a] Each experiment was performed in TCE with complex **4** (0.00506 M) and n-Bu_4NN_3 as cocatalyst (0.0098 M), TMC concentration = 0.98 M.

polymerization process. As can be readily seen, the ROP reaction ultimately becomes independent of [cocatalyst] loadings as would be expected. A double reciprocal plot of these data reveals a linear relationship with a limiting rate constant (k_{obsd}) of 0.059 h^{-1} at 120 °C.

The ring-opening polymerization of TMC was carried out over the temperature range 105–130 °C in order to obtain the activation parameters for this process. The rate constants of the ring-opening reaction, k_p, are listed in Table 10. The activation parameters $\Delta H^{\ddagger}$ and $\Delta S^{\ddagger}$ calculated from the Erying plot shown in Figure 14 were determined to be 74.1 ± 3.0 kJ/mol and −72.3 ± 2.3 J/mol·K, respectively. These parameters are consistent with a reaction pathway involving the attack of a nucleophilic center (polymer chain end) to a metal-bound cyclic carbonate (*vide infra*). The $\Delta G^{\ddagger}$ value of 101.9 kJ/mol at 110 °C for the ROP of TMC is quite similar to the comparable $\Delta G^{\ddagger}$ found for the copolymerization of oxetane and CO_2 of 107.6 kJ/mol. This small difference in $\Delta G^{\ddagger}$ for oxetane/CO_2 copolymerization and ring-opening polymerization of TMC clearly demonstrates that

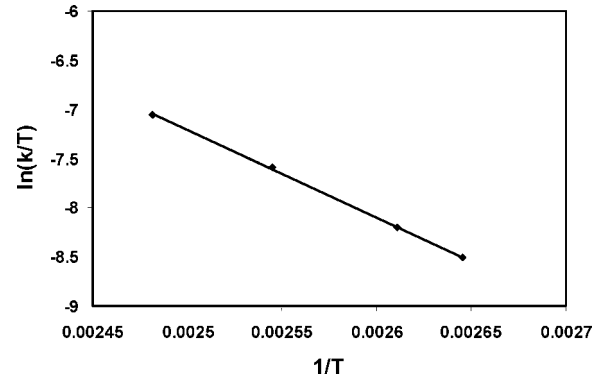

Figure 14. Eyring plot for the formation of poly(TMC) in the presence of complex **4**/n-Bu_4NN_3 catalyst system in TCE. Slope = −8910.7 with R^2 = 0.9997.

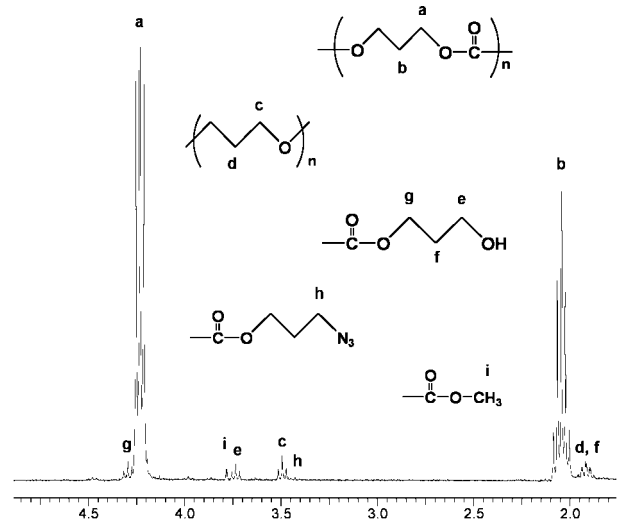

Figure 15. ^1H NMR spectrum in $CDCl_3$ of poly(TMC) obtained by way of oxetane/CO_2, in the presence of (salen)Cr(III)Cl/n-Bu_4NN_3 as the catalytic system. Polymer was purified from dichloromethane and 1 M HCl solution in methanol.

the two processes are energetically quite similar. Hence, the formation of polycarbonate from the oxetane and CO_2 coupling reaction could be occurring *via* two different or concurrent pathways, i.e., the intermediacy of TMC formation and subsequent polymerization and/or the direct enchainment of oxetane and CO_2. Indeed, *in situ* infrared spectroscopic monitoring of the copolymerization reaction suggests both pathways are operative (*vide supra*). Further studies detailed below based on monitoring of the coupling of oxetane and CO_2 by ^1H NMR spectroscopy, accompanied by end-group analysis of the low molecular weight copolymers produced, are designed to more definitively address this issue.

Further Mechanistic Insight into the Oxetane and Carbon Dioxide Coupling Process. As mentioned above, an inquiry of the mechanistic aspects of the oxetane and carbon dioxide coupling reaction was undertaken utilizing ^1H NMR spectroscopy studies which should provide a better assessment of the role of trimethylene carbonate in this process. The copolymerization reactions were performed under identical conditions as those previously described herein, i.e., complex **4**/2 equiv of n-Bu_4NN_3, 35 bar CO_2, 110 °C, and catalyst loading of 0.28 mol %. For these investigations, analysis of the reaction mixture was done by manually sampling a small aliquot withdrawn from the stainless steel reactor with subsequent quenching of the

Scheme 2

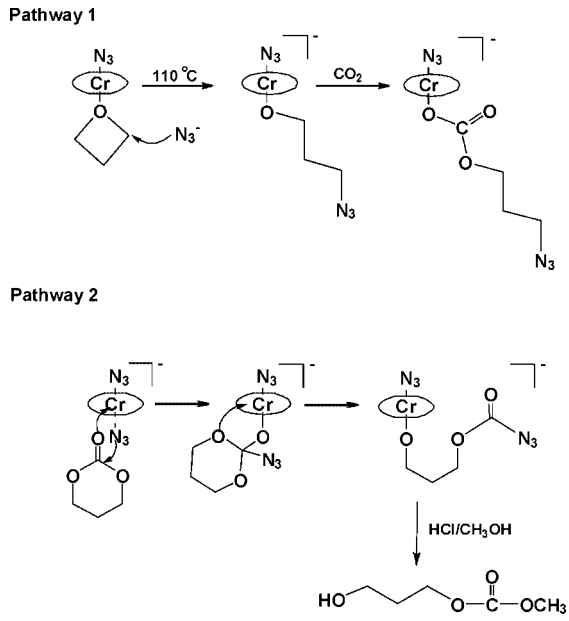

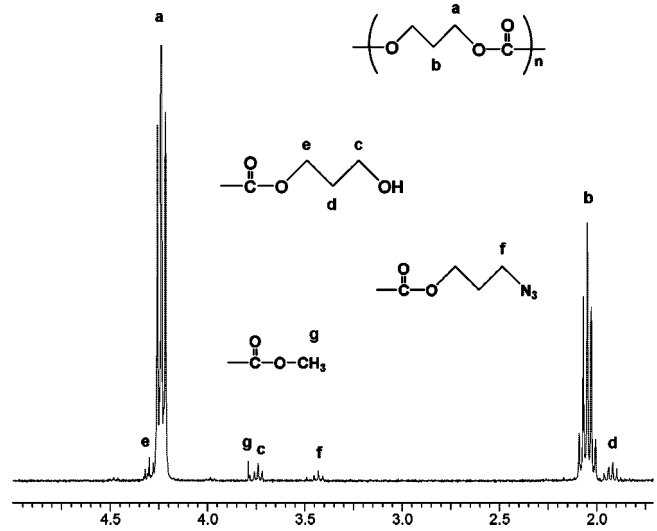

Figure 16. ^{1}H NMR spectrum in $CDCl_3$ of poly(TMC) sample obtained by ROP of TMC in the presence of (salen)Cr(III)Cl/*n*-Bu_4NN_3 as the catalytic system. Polymer was purified from dichloromethane and 1 M HCl solution in methanol.

reaction's progress by cooling the solution to 10 °C. As was observed during this process by *in situ* infrared spectroscopic monitoring, formation of TMC was detected prior to poly(TMC) formation. That is, the initial formation of TMC was detected within 30 min by the appearance of a triplet at 4.43 ppm and a quintet at 1.98 ppm, with its consequent consumption to produce polycarbonate. After 4 h of reaction no TMC was observed in the reaction mixture. Hence, it is apparent that in the early stages of the reaction a portion of the polycarbonate results from the ring-opening of trimethylene carbonate. This observation, coupled with the presence of some ether linkages in the copolymer, strongly supports the conclusions that both oxetane/CO_2 enchainment and TMC ring-opening are occurring simultaneously. End-group analyses of the polycarbonates produced from oxetane/CO_2 copolymerization and ROP of TMC were carried out in an effort to further corroborate these claims.

Figure 15 illustrates the ^{1}H NMR spectrum of a purified polycarbonate sample obtained from the copolymerization of oxetane and carbon dioxide. *Purification of the copolymer was achieved by precipitation from a dichloromethane solution with 1 M HCl in methanol, followed by vacuum drying.* In $CDCl_3$ the copolymer exhibits two major signals at 4.23 ppm (t, 4H, $^3J_{HH}$ = 6.3 Hz, $-OCH_2$) and 2.05 ppm (quint, 2H, $^3J_{HH}$ = 5.9 Hz, $-CH_2$). Ether linkages were observed in the copolymer at 3.50 ppm (t, 4H, $^3J_{HH}$ = 5.9 Hz, $-OCH_2$) and 1.90 ppm (quint, 2H, $^3J_{HH}$ = 5.9 Hz, $-CH_2$). A $-CH_2OH$ end group was observed before and after purification of the copolymer sample. These latter proton resonances appeared at 4.29 ppm (t, 2H, $^3J_{HH}$ = 6.0 Hz, $-CH_2$), 3.73 ppm (t, 2H, $^3J_{HH}$ = 6.3 Hz, $-CH_2$), and 1.90 ppm (t, 2H, $^3J_{HH}$ = 5.9 Hz, $-CH_2$).[17,20,36] The presence of an organic azide end group ($-CH_2N_3$) was also seen in the ^{1}H NMR spectrum of the copolymer at 3.43 ppm (t, 2H, $^3J_{HH}$ = 6.3 Hz, $-CH_2$), with the other two resonances being obscured by the intense polymer signals at 4.23 and 2.05 ppm. This assignment was made based on the ^{1}H NMR spectrum in $CDCl_3$ of a model compound (3-azido-propan-1-ol), which showed signals at 3.74 ppm (t, 2H, $^3J_{HH}$ = 6.0 Hz, $-CH_2OH$), 3.47 ppm (t, 2H, $^3J_{HH}$ = 6.6 Hz, $-CH_2N_3$), 1.83 ppm (quint, 2H, $^3J_{HH}$ = 5.9 Hz, $-CH_2CH_2CH_2$), and 1.77 ppm (s, 1H, $-OH$). In addition, the infrared spectrum of this copolymer exhibited an organic azide ν_{N_3} mode at 2100 cm^{-1} in TCE. Finally, the polycarbonate displayed a ^{1}H NMR resonance at 3.79 ppm (s, 3H) attributed to the $-OC(O)OCH_3$ end group resulting from methanolysis of the original $-OC(O)N_3$ end group following copolymer purification from MeOH.[36]

Based on the above observations we can conclude that two initiation pathways are operative following the initial generation of some trimethylene carbonate *via* a back-biting process involving the carbonate species afforded from Pathway 1 (Scheme 2).

In a similar fashion, a low molecular weight polycarbonate obtained from the ring-opening polymerization of trimethylene carbonate was analyzed by ^{1}H NMR spectroscopy. Figure 16 illustrates the ^{1}H NMR spectrum of the resulting poly(TMC) sample in $CDCl_3$, which exhibits, as expected, two major resonances at 4.23 ppm (t, 4H, $^3J_{HH}$ = 6.0 Hz, $-OCH_2$) and 2.05 ppm (quint, 2H, $^3J_{HH}$ = 6.3 Hz, $-CH_2$). *Importantly, no ether linkages were observed in this polycarbonate.* A $-CH_2OH$ end group was observed before and after polymer purification, with ^{1}H NMR resonances appearing at 4.29 ppm (t, 2H, $^3J_{HH}$ = 6.0 Hz, $-CH_2$), 3.73 ppm (t, 2H, $^3J_{HH}$ = 6.0 Hz, $-CH_2$), and 1.90 ppm (quint, 2H, $^3J_{HH}$ = 6.3 Hz, $-CH_2$). The presence of an organic azide end group was also seen in the polymer sample at 3.43 ppm (t, 2H, $^3J_{HH}$ = 6.3 Hz, $-CH_2N_3$) and 2100 cm^{-1} in the ^{1}H NMR and infrared spectra, respectively. Similarly, the presence of an $-OC(O)OCH_3$ end group at 3.79 ppm (s, 3H) was observed following polymer purification from methanol.

The latter observations, i.e., the presence of $-CH_2N_3$ and $-OC(O)OCH_3$ end groups in the polymer produced from TMC, established that the ring-opening of TMC under these catalytic conditions occurs *via* both acyl−oxygen and alkyl−oxygen bond cleavage modes (Scheme 3). Previously, we and others have

(36) Kricheldorf, H. R.; Weegen-Schulz, B. *Polymer* **1995**, *36*, 4997–5003.
(37) Ling, J.; Shen, Z.; Huang, Q. *Macromolecules* **2001**, *34*, 7613–7616.
(38) It is however felt that only one copolymer chain grows from a single chromium center. In other words the second azide ligand in the anionic chromium species is probably displaced by oxetane following the ring-opening process, with subsequent incorporation into the copolymer as an end group. Evidence for this is seen in Figure 2, where upon complete ring-opening of oxetane (spectrum C) there is *no* metal bound or free azide present in the spectrum.

Scheme 3

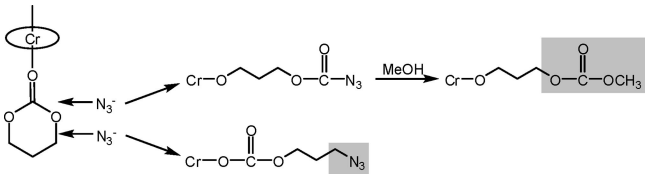

Scheme 4

Initiation Step

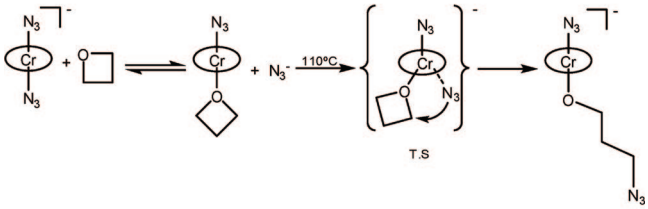

Chain Propagation

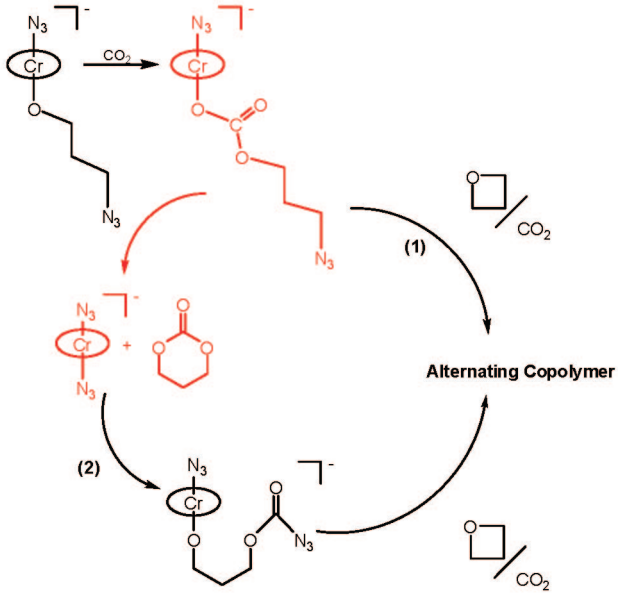

Chain Termination

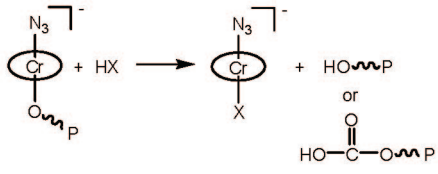

reported that the mechanism for ring-opening polymerization of TMC occurs exclusively by acyl−oxygen bond cleavage.[12,16,37] However, the presence of an organic azide end group in the poly(TMC) sample obtained by this route utilizing the (salen)-CrCl/*n*-Bu_4NN_3 catalytic system suggests that under these higher temperatures the ring-opening polymerization of TMC could also be initiated by an alkyl−oxygen bond cleavage.

Scheme 4 summarizes the proposed mechanistic aspects for the copolymerization of oxetane and carbon dioxide based on our current experimental findings. Although we have indicated only one of the chromium bound azide ligands taking part in the reaction, both are most likely involved.[38] As pointed out in the transition state illustrated in Scheme 4 of the initiation step, the azide ion has some association with the chromium center during the ring-opening process, as would be expected for the growing copolymer chain. Following the initial ring-opening step and CO_2 insertion into the resultant chromium−oxygen bond, two pathways are open for the intermediate. Route (1) involves consecutive additions of oxetane and CO_2 to yield the alternating copolymer, whereas route (2) leads to TMC formation by a back-biting process with ring closure. Once TMC is formed it can enter the copolymer chain by a coordination−insertion mechanism. The portion of route (2) shown in red should be highly dependent on the nature of the anionic leaving group. *Indeed, we have noted for the bromide ion that this pathway is competitive with oxetane enchainment and may provide a means for tuning the selectivity of the two pathways for poly(TMC) formation.* An advantage of proceeding exclusively *via* route (2) is the absence of ether linkages in the afforded polycarbonate.

Concluding Remarks

In summary, we have shown that chromium(III) salen complexes along with anionic initiators are effective catalysts for the copolymerization of oxetane and carbon dioxide. Optimization of the chromium catalyst was achieved utilizing a salen ligand with *tert*-butyl substituents in the 3,5-positions of the phenolate rings and a cyclohexylene backbone in the diimine, along with an azide ion as an initiator. Structural studies showed that oxetane binding to the chromium center occurred with little changes in its metric parameters as compared with the free cyclic ether. In particular, it remained nonplanar with the dihedral angle of the planes C−O−C and C−C−C being 10.5° at 110 K. Kinetic measurements performed employing *in situ* infrared monitoring showed the oxetane/CO_2 coupling reaction to be first-order in oxetane, metal catalyst, and anionic initiator, with the latter exhibiting zero-order dependence at high concentrations. Furthermore, both infrared and ^{1}H NMR spectroscopy demonstrated the production of trimethylene carbonate in the early stages of the copolymerization process. Nevertheless, the presence of ether linkages in the copolymer clearly revealed that direct enchainment of oxetane and CO_2 into the growing polymer chain occurs. The similarity of the free energy of activation of the copolymerization reaction of CO_2 and oxetane and the ring-opening polymerization of trimethylene carbonate supports these findings. Additional studies are being directed at tuning the selectivity of the oxetane and CO_2 coupling process for cyclic carbonate or copolymer by altering the anionic initiator or by using metal salen derivatives in oxidation state +2.

Acknowledgment. We gratefully acknowledge the financial support from the National Science Foundation (CHE-0543133) and the Robert A. Welch Foundation (A-0923).

Supporting Information Available: Experimental details for the synthesis and polymerization reactions, and X-ray crystallographic files in CIF format for the structure determination of complexes **5** and **6**. ^{1}H NMR spectra of low molecular weight polymers produced from oxetane/CO_2 and TMC for reactions catalyzed by complex **4** in the presence of *n*-Bu_4NCl. This material is available free of charge via the Internet at http://pubs.acs.org.

JA800302C